Published in final edited form as:
Curr Cardiovasc Imaging Rep. 2013 February 1; 6(1): 11–24. doi:10.1007/s12410-012-9177-x.

Gadolinium-Based Contrast Agents for Vessel Wall Magnetic Resonance Imaging (MRI) of Atherosclerosis

Claudia Calcagno,
Translational and Molecular Imaging Institute, Mount Sinai School of Medicine, One Gustave L. Levy Place, Box 1234, New York, NY 10029, USA, Department of Radiology, Mount Sinai School of Medicine, One Gustave L. Levy Place, New York, NY 10029, USA

Sarayu Ramachandran,
Translational and Molecular Imaging Institute, Mount Sinai School of Medicine, One Gustave L. Levy Place, Box 1234, New York, NY 10029, USA, Department of Radiology, Mount Sinai School of Medicine, One Gustave L. Levy Place, New York, NY 10029, USA

Antoine Millon,
Translational and Molecular Imaging Institute, Mount Sinai School of Medicine, One Gustave L. Levy Place, Box 1234, New York, NY 10029, USA, Department of Radiology, Mount Sinai School of Medicine, One Gustave L. Levy Place, New York, NY 10029, USA

Philip M. Robson,
Translational and Molecular Imaging Institute, Mount Sinai School of Medicine, One Gustave L. Levy Place, Box 1234, New York, NY 10029, USA, Department of Radiology, Mount Sinai School of Medicine, One Gustave L. Levy Place, New York, NY 10029, USA

Venkatesh Mani, and
Translational and Molecular Imaging Institute, Mount Sinai School of Medicine, One Gustave L. Levy Place, Box 1234, New York, NY 10029, USA, Department of Radiology, Mount Sinai School of Medicine, One Gustave L. Levy Place, New York, NY 10029, USA

Zahi Fayad
Translational and Molecular Imaging Institute, Mount Sinai School of Medicine, One Gustave L. Levy Place, Box 1234, New York, NY 10029, USA

Department of Radiology, Mount Sinai School of Medicine, One Gustave L. Levy Place, New York, NY 10029, USA

Zahi Fayad: zahi.fayad@gmail.com

Abstract

Cardiovascular disease due to atherosclerosis is the number one killer in the Western world, and threatens to become the major cause of morbidity and mortality worldwide. It is therefore paramount to develop non-invasive methods for the detection of high-risk, asymptomatic individuals before the onset of clinical symptoms or events. In the recent past, great strides have been made in the understanding of the pathological mechanisms involved in the atherosclerotic cascade down to the molecular details. This has allowed the development of contrast agents that can aid in the in vivo characterization of these processes. Gadolinium chelates are among the contrast media most commonly used in MR imaging. Originally used for MR angiography for the

Correspondence to: Zahi Fayad, zahi.fayad@gmail.com.

Disclosure No potential conflicts of interest relevant to this article were reported.

detection and quantification of vascular stenosis, more recently they have been applied to improve characterization of atherosclerotic plaques. In this manuscript, we will briefly review gadolinium-chelates (Gd) based contrast agents for non-invasive MR imaging of atherosclerosis. We will first describe Gd-based non-targeted FDA approved agents, used routinely in clinical practice for the evaluation of neovascularization in other diseases. Secondly, we will describe non-specific and specific targeted contrast agents, which have great potential for dissecting specific biological processes in the atherosclerotic cascade. Lastly, we will briefly compare Gd-based agents to others commonly used in MRI and to other imaging modalities.

Keywords

Atherosclerosis; Imaging; Gadolinium; Gd; Contrast agent; Magnetic resonance imaging; MRI; CE-MRI; DCE-MRI; Non-specific contrast agents; Specific non-targeted contrast agents; Specific targeted contrast agents

Introduction

Cardiovascular disease due to atherosclerosis is the leading cause of morbidity and mortality worldwide [1]. Atherosclerosis is a progressive systemic disease of medium and large arteries, which involves the accumulation of lipids, cells and fibrous tissue (plaques) in the arterial vessel wall. Its clinical history can be very diverse, with some individuals experiencing a slow, progressive, symptomatic disease, while others are asymptomatic and then present with acute life-threatening clinical manifestations, such as myocardial infarction, stroke and sudden death [1]. In recent years it has become clearer that traditional population risk factors and the degree of luminal stenosis cannot successfully identify "vulnerable" patients at high-risk for severe cardiovascular events [2-4].

With a better understanding of the histological and molecular characteristics of high-risk vulnerable plaques (Fig. 1a), novel non-invasive imaging techniques have been developed to identify high-risk individuals before the occurrence of clinical manifestations [4, 5••].

Many of the stages of plaque formation have been investigated using non-invasive magnetic resonance imaging (MRI) [6, 7]. Non-contrast enhanced MRI with different weightings (T1, T2 and PD) exploits the native relaxation properties of plaque components to differentiate them [4]. Differently, contrast enhanced MRI uses non-targeted or targeted contrast agents to modify these native relaxation properties in order to aid in the detection of hallmarks of vulnerability. Several contrast media can be used to characterize atherosclerotic plaques. Gadolinium (Gd) is one of the contrast agents most commonly used in MR imaging. As free gadolinium is toxic [8], its clinical formulations contain chelating agents. Gadolinium based MR contrast agents act by shortening the longitudinal relaxation time (T1) and cause signal enhancement in areas of accumulation which can be detected using T1 weighted MR sequences [9]. These agents are routinely used in clinical practice to quantify the extent and characteristics of tissues neovascularization in several physiological and pathological instances (such as tumors) and its changes after therapeutic intervention [10].

In the context of atherosclerosis, FDA approved Gd based contrast agents are routinely used for contrast enhanced (CE) MR angiography, which is nowadays considered the most accurate modality for the detection of severe (70–99 %) carotid stenosis [11]. However, these agents not only delineate the vessel lumen, but also extravasate in the vessel wall and cause signal enhancement in atherosclerotic plaques (Fig. 1b). The pattern of enhancement depends on plaque neovascularization, neovessels permeability, extracellular matrix content and presence or absence of a fibrous cap (Fig. 1b), which are important components of

vulnerable plaques [12••]. As an alternative, Gd can be used to create contrast agents that actively or passively target specific processes of the atherosclerotic cascade. For example, Gd-based specific agents have been described to target: 1) adhesion molecules (integrins, selectins, $\alpha v\beta 3$) expressed on the diseased the vessel wall and neovessel endothelium; 2) macrophages, through their scavenger receptor; 3) elastin in the extra-cellular matrix; 4) proteinases 5) thrombus and fibrin 6) apoptosis and so on [9, 12••] (Fig. 1a and b).

In this review article we focus on the description of non-invasive magnetic resonance imaging techniques with the use of untargeted and targeted gadolinium based contrast agents for the detection and characterization of vulnerable atherosclerotic plaques.

Non-Targeted Gadolinium Based Contrast Agents

Contrast Enhanced (CE) MRI

As mentioned above, Gd based FDA approved contrast agents are routinely used in CE-MRA studies for stenosis quantification, but are also used in pre-clinical and clinical studies to improve plaque identification and characterization, in particular with respect to the detection of neovessels, loose matrix, fibrous cap and intra-plaque hemorrhage [13]. In CE-MRI, after acquisition of baseline, non-contrast enhanced images a Gd based contrast agent is injected. Contrast enhanced imaging is then performed at an optimal time (5–10 minutes depending on the contrast agent) after injection [13-15], by acquiring one imaging time point in the same way as it was acquired at baseline. By comparing the baseline and post contrast acquisition, the pattern and intensity of tissue enhancement can be characterized.

Pre-clinical studies found that enhancement after injection of Gd diethylenetriaminepentaacetic acid (DTPA) was significantly higher in atherosclerotic than in normal vessel walls [16]. Enhancement was found to correlate with plaque neovascularization and inflammation [17-19] and to be higher in lipid-rich quadrants compared with fibrous quadrants and in macrophage-rich compared to macrophage-poor plaques [16]. Using multiple regression analysis, it was shown that macrophage-rich areas and neovessel density are independently associated with plaque enhancement [16].

In clinical studies, FDA approved Gd based contrast agents have been extensively used for vessel wall delineation [20] and to improve plaque characterization in the carotid arteries. Several studies demonstrated that contrast enhanced MRI with Gd-DTPA was able to differentiate plaque fibrous cap and lipid core, better than conventional T2 weighted imaging (Fig. 2a and b) in human carotid arteries [14]. Additionally, highly enhancing fibrous regions identified by CE MRI were shown to correspond to neo-vessels and inflammatory cell rich areas by histology [21, 22]. No difference was found in the pattern of enhancement depending upon contrast agent type. [23] This technique was found to be as reliable as non-contrast-enhanced MRI in a multi-center clinical trial setting [24] and has been recently used in the BioImage high-risk plaque initiative for primary prevention in asymptomatic subjects at high-risk for cardiovascular events [25, 26]. Recently CE MRI has also been used during intra-vascular MRI to improve signal-to-noise ratio (SNR) for imaging deep arteries (such as the iliacs) in human subjects [27]. Additionally CE MRI with Gd-DTPA was used to image the coronary artery wall in subjects after acute myocardial infarction (AMI) and subjects without coronary artery disease [28] and showed higher contrast-to-noise ratio (CNR) in the coronary vessel wall of subjects with AMI 6 days after infarction compared with normal subjects, followed by a decrease in CNR three months after infarction, paralleled by a decline in C-reactive protein (CRP). In the basilary artery, a study [29] investigated the relationship between luminal narrowing and Gd-DTPA enhancement after recent stroke and found higher wall enhancement in narrowed arteries in both patients with recent infarction and in patients with subsequent ischemic events.

Despite the numerous pre-clinical and clinical studies using Gd based agents listed above, the clinical meaning of plaque enhancement is not completely understood. For example, while it is intuitive that non-targeted agents should accumulate in neovessels rich areas [14, 21, 22], their presence has also been described, (albeit with a different pattern of enhancement) in the loose extra-cellular matrix, another marker of vulnerability [15, 21]. This ambiguity makes it difficult to interpret the clinical meaning of CE MRI and its implication for patients risk stratification.

Dynamic Contrast Enhanced (DCE) MRI

DCE-MRI can provide additional information with respect to CE MRI, as it tracks contrast agent uptake in atherosclerotic plaques with a dynamic acquisition (as opposed to the static nature of CE-MRI). DCE-MRI consists of the rapid serial acquisition of MR images during the injection of FDA approved Gd based contrast agents. Contrast agents extravasate through the microvasculature into the tissue extra-cellular space. The rate of accumulation of contrast agents and the characteristics of tissues enhancement depend on the fraction of the tissue occupied by the microvasculature (fractional plasma volume, v_p), vascular flow and permeability (K^{trans}), and the fraction of extra-vascular extra-cellular space (v_e) [10] (Fig. 3). These physiological parameters can be derived from time-concentration curves by the use of standard kinetic modeling analyses [10].

In the last ten years DCE-MRI has been employed to quantify neovascularization in atherosclerosis. Using spoiled gradient echo (SPGR) based “bright blood” (without blood suppression) MR sequences it was demonstrated that the kinetic parameters fractional plasma volume (v_p) and K^{trans} (expressing flow/permeability) correlate significantly with neovessels density in carotid plaques of subjects who underwent carotid endarterectomy (CEA) (Fig. 2c) [30, 31] with K^{trans} correlating also with macrophages density and extracellular matrix content. These associations were found to be independent of the contrast agent used [23]. K^{trans} was also found to be higher in smokers [31, 32], in subjects with low levels of HDL [31], in patients undergoing CEA (or with carotid plaques classified as AHA type VI) with respect to patients with moderate disease, and in subjects with high BMI, diastolic blood pressure (DBP), and CRP [32]. K^{trans} was recently demonstrated to be a good index to track changes in plaque neovascularization/permeability after therapeutic intervention, as a reduction in K^{trans} was demonstrated in human subjects after one year of lipid lowering therapy, independent of a reduction in lipid right necrotic core or circulating levels of CRP [33]. Despite these encouraging results, SPGR based bright blood DCE-MRI acquisitions are only suited for the characterization of lesions thicker than 2 mm, because of the close proximity of the enhancing vessel lumen, which makes it challenging to trace the contours of a thinner vessel wall [34].

As an alternative, so called “black blood” MR sequences, where the signal coming from the vessel lumen is suppressed, can be used to perform DCE-MRI of human lesions less than 2 mm thick or in animal models [34]. Blood suppression is commonly achieved by exploiting the native black blood properties of the spin echo (SE) acquisition kernel, often coupled with additional techniques, such as double [35] or quadruple [34] inversion recovery. Suppression of the blood signal precludes the use of kinetic modeling to analyze DCE-MRI data. Alternatively, enhancements curves can be analyzed using non-model based parameters, such as uptake slope, time to peak and area under the curve (AUC). These quantities have the advantage of being easier to calculate than model-based parameters. However their relationship with well defined physiological quantities is unclear [36].

Black blood DCE-MRI was used in the abdominal aorta [37, 38] of ApoE(–/–) mice to investigate vascular permeability. Maximal vessel wall enhancement was demonstrated between 15–30 minutes after injection, with enhancement varying depending on the age of

the animals (higher for animals 4–8 weeks old, but lower for animals that were 16 weeks old). Subsequently, a significant positive relationship between the non-model parameter AUC and plaque neovascularization was demonstrated in aortic plaques of atherosclerotic rabbits [35]. The reproducibility of AUC was also investigated in this setting [39] and was found to be excellent. Additionally, DCE-MRI was used in combination with FDG-PET (a technique able to quantify vascular inflammation) as a read-out for anti-atherosclerotic therapy in atherosclerotic rabbits in several studies [40-43]. A significant reduction in AUC was demonstrated 48 hours after the injection of liposomal corticosteroids [12••, 40] after 3 months of treatment with the oral antidiabetic pioglitazone [42] (Fig. 2d and e), atorvastatin and using a novel liver X receptor (LXR) agonist [43].

As an alternative to non-model based parameters, reference region models can be used to analyze black blood DCE-MRI data. Using one such approach, K^{trans} was found to increase in aortic plaques of atherosclerotic rabbits between 3 and 6 months after diet injury [34], and showed a significant correlation with macrophage content by histology.

Lastly, black blood DCE-MRI was recently employed as a tertiary endpoint in the dal-PLAQUE clinical trial, evaluating the efficacy of the CETP inhibitor dalcetrapib. In agreement with other imaging endpoints (non-contrast MRI and FDG-PET), DCE-MRI showed no changes in plaque perfusion after intervention [44, 45].

Targeted Gadolinium Based Contrast Agents

Targeted Gd based contrast media can be divided into non-specific and specific agents. Non-specific targeted agents exploit the increased permeability of plaque neovessels to enter and permeate atherosclerotic plaques, in what is called the enhanced permeability and retention (EPR) effect [12••, 46]. Specific, targeted contrast agents can be either synthetic or natural agents with well-defined molecular targets either on the neovasculature or in the plaque itself [12••]. A review of the most common Gd based targeted agents follows.

Non-Specific Targeted Gadolinium Based Contrast Agents

Blood pool, non-specific agents enter the plaque through passive targeting due to the increased permeability of the neovasculature in vulnerable lesions (EPR effect) [12••, 46]. Gadofosveset and gadolfluorine M are examples of blood pool agents that have been used to improve atherosclerotic plaques characterization. Studies in atherosclerotic rabbits [47, 48] showed higher enhancement using gadofosveset [47] (Fig. 4a-c) or an albumin binding agent (B-22956/1, Fig. 4d) [48] with respect to Gd-DTPA, and correlated enhancement with plaque neovascularization and macrophages density. Using ApoE–/– mice [49] it was demonstrated that enhancement due to gadofosveset increases with plaque progression and is lower in statin treated ApoE(–/–) mice (Fig. 4e). The uptake of gadofosveset was correlated with Evans blue staining, suggesting that uptake occurs in regions of increased vascular permeability. In a clinical setting, gadofosveset was used to characterize human carotid plaques [50] and showed higher signal enhancement in plaques from symptomatic compared with asymptomatic patients and was significantly associated with intra-plaque albumin content by histology, but not with other plaque components.

Gadofluorine M was also shown to accumulate in aortic [51-53] and femoral [54] plaques of atherosclerotic rabbits and in the carotid arteries of balloon injured Yucatan miniswines [55]. Enhancement was shown to correlate with plaque macrophage content and neovascularization [51-53]. A strong spatial correlation between lipid rich areas in histological sections and MR signal enhancement after injection of gadofluorine M was also demonstrated in aortic plaques of balloon injured New Zealand White (NZW) rabbits, thus suggesting an affinity of this contrast agent for lipid-rich vulnerable plaques [56]. Further

investigations [57] have shed more light on the mechanisms of plaque enhancement by gadofluorine M: this contrast agent binds to albumin in the circulation, then penetrates the atherosclerotic plaque while bound to albumin and accumulates within the extracellular, fibrous parts of the plaque and in the fibrous cap by binding to collagens, proteoglycans and tenascin, with the same affinity as to albumin. The authors therefore hypothesized that gadofluorine M might enable the detection of thin-cap fibroatheromas [57].

Specific Targeted Gadolinium Based Contrast Agents

Gd based specific targeted agents have been described to investigate virtually every process and molecule involved in the atherosclerotic cascade. Below we describe some of the most relevant agents developed in this category and their applications and provide a summary in Table 1 for clarity.

Endothelial dysfunction and the subsequent entry of lipoproteins into the vessel wall are the initial stages of plaque formation. Once in the vessel wall, lipoproteins get oxidized and elicit an inflammatory response which is responsible for the progression of atheromas. Oxidized lipoproteins can be specifically targeted using Gd-based contrast agents. For example Gd based specific probes targeted at the oxidized low-density lipoprotein receptor (LDLR) LOX-1 have been developed [58] and showed significant Gd enhancement in atherosclerotic plaques in LDLR(–/–) mice. The LOX-1 probe bound preferentially to the plaque shoulder, a region with vulnerable plaque features, including extensive LOX-1 expression, macrophage accumulation, apoptosis, and matrix metalloproteinase-9 (MMP-9) expression. Using another approach, Gd micelles containing murine (MDA2 and E06) or human (IK17) antibodies that bind unique oxidation-specific epitopes were developed [59] and showed significant enhancement of macrophages rich areas of atherosclerotic plaques in ApoE(–/–), but not wild type mice.

Adhesion molecules such as P- and E-selectin, vascular cell adhesion molecule-1 (VCAM-1) and intercellular adhesion molecule-1 (ICAM-1) are pivotal in the development of atherosclerosis. They facilitate mononuclear leukocyte recruitment to the activated endothelium and their subsequent transmigration into the subendothelial space. ICAM-1 and P-selectin have been used as targets for the development of novel Gd based contrast agents. Studies in vitro [60] demonstrated that Gd based agents functionalized with anti-ICAM-1 antibodies for MRI of endothelial ICAM-1 expression induced signal enhancement in cells activated by TNFα, with respect to controls. Using another approach [38, 61] others grafted key chemical groups involved in the interaction between P-selectin and its endogenous ligand (PSGL-1) onto Gd-DOTA (F-P717) to assess arterial wall inflammation in ApoE(–/–) mice and found that F-P717 caused significant signal enhancement of MRI in the abdominal aortic wall of ApoE(–/–) mice, but not of control mice. The integrin αvβ3 is highly expressed by medial and intimal smooth muscle cells and by endothelial cells of neovessels in atherosclerotic plaques. αvβ3 is a good example of the development of novel targeted contrast media to non-invasively assess angionenesis in early atherosclerosis and as a vehicle for drug-delivery and read-out of anti-angiogenic therapy [62-65]. Using a paramagnetic agent targeted to αvβ3 [63] successful targeting of plaque neovascularization in atherosclerotic rabbits [63] and mice [66] animal model was shown. In atherosclerotic rabbits a decrease in MRI enhancement was demonstrated after administration of the same contrast agent incorporating fumagillin, an anti-angiogenic drug [62] (Fig. 5a and b). A marked and sustained anti-angiogenic response was achieved when delivering atorvastatin and 2 doses of αvβ3 targeted fumagillin nanoparticles (at 0 and 4 weeks) [64]. Conversely, higher signal enhancement was found in animals treated with L-arginin, which was found by histology to promote a denser pattern of microvasculature [65].

Macrophages are important in atherogenesis and in the formation of vulnerable plaques, as they participate in the inflammatory response that can lead to plaque rupture. Examples of Gd based contrast media aimed at quantifying macrophages plaque burden are agents targeted to the macrophage scavenger receptor (MSR). MSR targeted Gd based immunomicelles [67, 68] and nanoparticles [69] have been investigated and showed a strong correlation between plaque macrophage content and signal enhancement by MRI. Paramagnetic phosphatidylserine vesicles containing cholesterol ester with a free carboxylic acid [70, 71] function have also been used for targeted imaging of macrophages in atherosclerotic rabbits and caused protracted enhancement by MRI and colocalization with arterial macrophages, which was not seen with control vesicles. Lipoproteins are naturally targeted to plaque macrophages and are therefore an ideal candidate for their detection using imaging. Functionalized LDL particles [72] have been described for the in vivo detection of atherosclerotic plaques and showed significant signal enhancement in atherosclerotic mice. Recombinant [73, 74] and fully synthetic [75] HDL-like nanoparticles have also been developed and exhibited signal enhancement in macrophages rich plaque of atherosclerotic mice (Fig. 5g and h). When describing plaque macrophages targeting by MRI contrast agents, it is worthwhile to mention other MR contrast media commonly used for this purpose, such as iron oxides. Small (SPIO) and ultrasmall (USPIO) iron oxides exhibit T2* shortening properties, which causes signal loss on T2* weighted sequences in areas of accumulation. In the early 2000s [76, 77] it was demonstrated that SPIOs and USPIOs are spontaneously phagocyted by plaque macrophages in atherosclerotic rabbits and in humans [78]. Since then, these agents have been extensively used for the detection of plaque macrophages. For example, SPIOs have recently been used in the “Atorvastatin Therapy: Effects on Reduction of Macrophage Activity (ATHEROMA)” trial to track prospectively the effect of high and low statin therapy on carotid plaque inflammation [79] (Fig. 6a and b). In addition to macrophages targeting, iron oxide nanoparticles have been used to create other contrast agents specifically targeted to other plaque components, such as adhesion molecules and cell apoptosis.

Cell apoptosis is also a marker of atherosclerotic plaque vulnerability and is therefore an important diagnostic and therapeutic target for imaging atherosclerosis. Apoptotic cells are characterized by the exposure of phosphatidylserine (PS) at their surface. Annexin A5-functionalized nanoparticles [80] have been developed for noninvasive MRI of PS exposing cells in atherosclerotic lesions. The accumulation of these particles in atherosclerotic ApoE(–/–) mice has been demonstrated by signal enhancement in T1 weighted MRI. Gd based liposomes enriched with PS (Gd-PS) were also shown to induce MR signal enhancement in macrophages. Using a novel approach base on phage display screening, a PS-specific peptide [81] was identified and used to design an MRI contrast agent, which was used as an in vivo reporter of apoptotic cells in ApoE(–/–) mice.

Plaque rupture correlates well with *myeloperoxidase* (MPO) secretion by activated neutrophils and macrophages in humans. In vitro [82] and in vivo studies in mice [83] and rabbits [84] used modified Gd-based agents as a paramagnetic sensors of MPO enzymatic activity. The in vivo studies found MR signal enhancement colocalized with MPO-rich areas infiltrated by macrophages on histopathological evaluation [84].

The extracellular matrix (ECM) plays an important role in the pathogenesis of atherosclerosis and plaque rupture. *Elastin* is an essential component of the ECM. ECM degradation can lead to plaque destabilization, whereas enhanced synthesis typically leads to vessel wall remodeling resulting in arterial stenosis or in-stent restenosis. Elastin binding agents (BMS-753951 [85], ESMA [86]) have been used to detect elastin in coronary arteries [85] and thoracic aorta [86] plaques of atherosclerotic pigs [85]. They found that strong enhancement by elastin targeted agents by MRI colocalized with elastic fibers, as confirmed

by electron microscopy and inductively coupled plasma mass spectroscopy (Fig. 5c-f). The clinical utility of this elastin atherosclerotic marker is unclear at this stage. Using a different approach, Gd polyethylene glycol (PEG)-micelles functionalized with tyrosine residues [87, 88] were also used for imaging atherosclerotic plaques in ApoE(–/–) mice and were shown to accumulate in plaques lipid-rich areas.

Matrix metalloproteinase (MMPs) are a family of enzymes that have been implicated in the vulnerability of plaques prone to rupture. The novel Gd-based MMP targeted agent P947 has been investigated both in vitro [89], ex-vivo in human carotid specimens [89] and in vivo in atherosclerotic mice [89, 90], and rabbits [89]. All these studies revealed high affinity of P947 for MMPs [89] and its preferential accumulation in MMP-rich versus MMP-poor plaques as detected by signal enhancement by MRI [89, 90]. Higher P947 accumulation was found in rabbits fed a 'high-fat' versus a 'low-fat' diet [90]. P947 was recently demonstrated to be able to detect in vivo not only MMPs, but also other proteinases activated in vulnerable plaques, such as angiotensin converting enzyme (ACE) and amino-peptidases N (APN) [91].

Thrombosis occurs after plaque rupture, because of the exposure of the pro-thrombotic environment of the lipid core to the circulating blood. Fibrin targeted, Gd-based agents (Gd-DTPA-BOA [92], Gd-DTPA-phosphatidylethanolamine (PE) [93], EP-2104R [94], EP-1242 [95], EP-1240 [96], FTCA [97]) have been described for in vivo imaging of thrombus surfaces and fibrin for the early detection of vascular micro-thrombi. Significant signal enhancement in thrombi was detected in diseased mice arteries regardless of their size, location, and age, while no enhancement was seen in control arteries, and late stage plaques exhibiting the highest enhancement, ex vivo fibrin staining and gadolinium concentration [97].

Conclusions and Future Directions

Gd-chelates are among the contrast agents most commonly used for MR imaging. They have a T1 shortening effect and cause signal enhancement in T1W sequences in areas of accumulation [9].

Albeit being commonly used in contrast enhanced (CE) MR angiography for the evaluation of luminal stenosis, FDA approved non-targeted contrast agents also enter the plaque and accumulate in areas of neovascularization or loose matrix. CE vessel wall MRI has been proven superior to conventional non-contrast enhanced MR imaging for vessel wall delineation and detection of different plaque components (such as fibrous cap) in human subjects (Fig. 2a and b). Dynamic contrast enhanced (DCE) MRI provides more quantitative information about plaque neovascularization and permeability [10] (Fig. 2c-e). Together with non-contrast enhanced MRI and 18F-FDG PET/CT (for the quantification of vascular inflammation), DCE-MRI has now been used as a surrogate endpoint in clinical drug trials. Using these novel imaging modalities as endpoints will revolutionize drug development trials as it will allow for faster and cheaper drug screening using a lower number of subjects than required with traditional outcome approaches. However, it must be noted that DCE-MRI of atherosclerosis is particularly challenging, because of the high spatial and time resolution required for accurate quantification of plaque perfusion indices and the necessity for black blood acquisition for plaques less than 2 mm thick [34, 35]. For this reason DCE-MRI is still an area of active research, and it is likely that future developments in this field will give further insights on the physiological meaning of plaque perfusion indices as markers of vulnerability.

Non-specific targeted contrast agents enter the plaque through the neovasculature and reside in the extra-cellular matrix or lipid rich areas, by exploiting the enhanced permeability and retention effect (EPR) [46]. Their accumulation has been shown to correlate spatially with

neovessels [47, 48], macrophages and lipid rich areas by some [51, 52, 56], but not all, authors [15, 57] (Fig. 4). Targeted specific contrast agents enter the plaque and specifically interact with target molecules. In this manuscript we reviewed the most relevant examples of Gd-based contrast agents targeted to hallmarks of plaque vulnerability. Examples of their application can be found in Fig. 5. Although still confined mostly to pre-clinical applications, the potential and possibilities for these agents to improve plaque characterization and patients risk stratification in the future are endless. A good example of their potential is the development of a targeted contrast agent against the integrin $\alpha v\beta 3$ (Fig. 5a and b), which was described not only as a tool to detect plaque neovascularization, but also as a carrier for the delivery and anti-angiogenic therapy [63-65, 93]. Similarly, Gd labeled liposomes [40] and Gd-HDL [98, 99], have been used as drug carriers to atherosclerotic lesions in rabbits to improve therapeutic efficacy. This very novel approach is known as nanomedical theranostics, which consists in the application of nanoparticulate agents to allow diagnostic therapy, which is being developed in fields other than cardiovascular imaging (for example oncology) for image-guided, personalized, targeted treatment of disease [12••].

Non-specific and specific Gd based MR agents may be used in future clinical practice together with other MR techniques or other imaging modalities for a comprehensive, well-rounded evaluation of plaque vulnerability. Among these additional imaging modalities, it is worth mentioning 18F-FDG PET/CT which provides an effective read-out for plaque inflammation [100-105] (Fig. 6). A recent study explored the relationship between DCE-MRI perfusion indices and 18F-FDG uptake by PET/CT in the carotid and vertebral arteries of patients with suspected arteritis [106] and found a positive significant correlation between DCE-MRI perfusion indices and plaque FDG uptake by PET/ CT. As many of the molecular targets described above are linked to plaque inflammation and vulnerability, further investigations are needed to establish the complementary role of these different techniques in plaque characterization and patient risk stratification.

Acknowledgments

NIH/NHLBI R01 HL071021, R01 HL078667; NIH/NBIB R01 EB009638 and NIH/NHLBI Program of Excellence in Nanotechnology (PEN) Award, Contract #HHSN268201000045C.

References

Papers of particular interest, published recently, have been highlighted as:

•• Of major importance

1. Libby, P. The Pathogenesis, Prevention, and Treatment of Atherosclerosis. Vol. Chapter 241. New York: McGraw-Hill; 2012.
2. Virmani R, Burke AP, Farb A, Kolodgie FD. Pathology of the vulnerable plaque. J Am Coll Cardiol. 2006; 47(8 Suppl):C13–8. [PubMed: 16631505]
3. Fuster V, Moreno PR, Fayad ZA, Corti R, Badimon JJ. Atherothrombosis and high-risk plaque: part I: evolving concepts. J Am Coll Cardiol. 2005; 46(6):937–54. [PubMed: 16168274]
4. Fuster V, Fayad ZA, Moreno PR, Poon M, Corti R, Badimon JJ. Atherothrombosis and high-risk plaque: Part II: approaches by noninvasive computed tomographic/magnetic resonance imaging. J Am Coll Cardiol. 2005; 46(7):1209–18. [PubMed: 16198833]
5••. Sanz J, Fayad ZA. Imaging of atherosclerotic cardiovascular disease. Nature. 2008; 451(7181): 953–7. A review about the pathogenesis of atherosclerosis and imaging techniques to improve the diagnosis and characterization of cardiovascular disease. [PubMed: 18288186]

6. Degnan AJ, Young VE, Gillard JH. Advances in noninvasive imaging for evaluating clinical risk and guiding therapy in carotid atherosclerosis. Expert Rev Cardiovasc Ther. 2012; 10(1):37–53. [PubMed: 22149525]
7. Joshi FR, Lindsay AC, Obaid DR, Falk E, Rudd JH. Non-invasive imaging of atherosclerosis. Eur Heart J Cardiovasc Imaging. 2012; 13(3):205–18. [PubMed: 22277118]
8. Kaewlai R, Abujudeh H. Nephrogenic systemic fibrosis. AJR Am J Roentgenol. 2012; 199(1):W17–23. [PubMed: 22733927]
9. Briley-Saebo KC, Mulder WJ, Mani V, Hyafil F, Amirbekian V, Aguinaldo JG, et al. Magnetic resonance imaging of vulnerable atherosclerotic plaques: current imaging strategies and molecular imaging probes. J Magn Reson Imaging. 2007; 26(3):460–79. [PubMed: 17729343]
10. Tofts PS, Brix G, Buckley DL, Evelhoch JL, Henderson E, Knopp MV, et al. Estimating kinetic parameters from dynamic contrast-enhanced T(1)-weighted MRI of a diffusable tracer: standardized quantities and symbols. J Magn Reson Imaging. 1999; 10(3):223–32. [PubMed: 10508281]
11. Anzidei M, Napoli A, Zaccagna F, Di Paolo P, Saba L, Cavallo Marincola B, et al. Diagnostic accuracy of colour Doppler ultra-sonography, CT angiography and blood-pool-enhanced MR angiography in assessing carotid stenosis: a comparative study with DSA in 170 patients. Radiol Med. 2012; 117(1):54–71. [PubMed: 21424318]
12••. Lobatto ME, Fuster V, Fayad ZA, Mulder WJ. Perspectives and opportunities for nanomedicine in the management of atherosclerosis. Nat Rev Drug Discov. 2011; 10(11):835–52. A review about nanothecnology and its use for the diagnosis and treatment of atherosclerosis, with several examples on targeting mechanisms for cardiovascular disease. [PubMed: 22015921]
13. Wasserman BA. Advanced contrast-enhanced MRI for looking beyond the lumen to predict stroke: building a risk profile for carotid plaque. Stroke. 2010; 41(10 Suppl):S12–6. [PubMed: 20876485]
14. Wasserman BA, Smith WI, Trout HH 3rd, Cannon RO 3rd, Balaban RS, Arai AE. Carotid artery atherosclerosis: in vivo morphologic characterization with gadolinium-enhanced double-oblique MR imaging initial results. Radiology. 2002; 223(2):566–73. [PubMed: 11997569]
15. Millon A, Boussel L, Brevet M, Mathevet JL, Canet-Soulas E, Mory C, Scoazec JY, Douek P. Clinical and Histological Significance of Gadolinium Enhancement in Carotid Atherosclerotic Plaque. Stroke. 2012
16. Hur J, Park J, Kim YJ, Lee HJ, Shim HS, Choe KO, et al. Use of contrast enhancement and high-resolution 3D black-blood MRI to identify inflammation in atherosclerosis. JACC Cardiovasc Imaging. 2010; 3(11):1127–35. [PubMed: 21071000]
17. Phinikaridou A, Hallock KJ, Qiao Y, Hamilton JA. A robust rabbit model of human atherosclerosis and atherothrombosis. J Lipid Res. 2009; 50(5):787–97. [PubMed: 19141434]
18. Phinikaridou A, Ruberg FL, Hallock KJ, Qiao Y, Hua N, Viereck J, et al. In vivo detection of vulnerable atherosclerotic plaque by MRI in a rabbit model. Circ Cardiovasc Imaging. 2010; 3(3): 323–32. [PubMed: 20194634]
19. Steen H, Lima JA, Chatterjee S, Kolmakova A, Gao F, Rodriguez ER, et al. High-resolution three-dimensional aortic magnetic resonance angiography and quantitative vessel wall characterization of different atherosclerotic stages in a rabbit model. Invest Radiol. 2007; 42(9):614–21. [PubMed: 17700276]
20. Aoki S, Shirouzu I, Sasaki Y, Okubo T, Hayashi N, Machida T, et al. Enhancement of the intracranial arterial wall at MR imaging: relationship to cerebral atherosclerosis. Radiology. 1995; 194(2):477–81. [PubMed: 7824729]
21. Cai J, Hatsukami TS, Ferguson MS, Kerwin WS, Saam T, Chu B, et al. In vivo quantitative measurement of intact fibrous cap and lipid-rich necrotic core size in atherosclerotic carotid plaque: comparison of high-resolution, contrast-enhanced magnetic resonance imaging and histology. Circulation. 2005; 112(22):3437–44. [PubMed: 16301346]
22. Yuan C, Kerwin WS, Ferguson MS, Polissar N, Zhang S, Cai J, et al. Contrast-enhanced high resolution MRI for atherosclerotic carotid artery tissue characterization. J Magn Reson Imaging. 2002; 15(1):62–7. [PubMed: 11793458]

23. Kerwin WS, Zhao X, Yuan C, Hatsukami TS, Maravilla KR, Underhill HR. Contrast-enhanced MRI of carotid atherosclerosis: dependence on contrast agent. J Magn Reson Imaging. 2009; 30(1):35–40. [PubMed: 19557844]
24. Chu B, Zhao XQ, Saam T, Yarnykh VL, Kerwin WS, Flemming KD, et al. Feasibility of in vivo, multicontrast-weighted MR imaging of carotid atherosclerosis for multicenter studies. J Magn Reson Imaging. 2005; 21(6):809–17. [PubMed: 15906345]
25. Falk E, Sillesen H, Muntendam P, Fuster V. The high-risk plaque initiative: primary prevention of atherothrombotic events in the asymptomatic population. Curr Atheroscler Rep. 2011; 13(5):359–66. [PubMed: 21800090]
26. Muntendam P, McCall C, Sanz J, Falk E, Fuster V. The BioImage Study: novel approaches to risk assessment in the primary prevention of atherosclerotic cardiovascular disease–study design and objectives. Am Heart J. 2010; 160(1):49–57 e41. [PubMed: 20598972]
27. Larose E, Kinlay S, Selwyn AP, Yeghiazarians Y, Yucel EK, Kacher DF, et al. Improved characterization of atherosclerotic plaques by gadolinium contrast during intravascular magnetic resonance imaging of human arteries. Atherosclerosis. 2008; 196(2):919–25. [PubMed: 17391676]
28. Ibrahim T, Makowski MR, Jankauskas A, Maintz D, Karch M, Schachoff S, et al. Serial contrast-enhanced cardiac magnetic resonance imaging demonstrates regression of hyperenhancement within the coronary artery wall in patients after acute myocardial infarction. JACC Cardiovasc Imaging. 2009; 2(5):580–8. [PubMed: 19442944]
29. Lou X, Ma N, Ma L, Jiang WJ. Contrast-Enhanced 3T High-Resolution MR Imaging in Symptomatic Atherosclerotic Basilar Artery Stenosis. AJNR Am J Neuroradiol. 2012
30. Kerwin W, Hooker A, Spilker M, Vicini P, Ferguson M, Hatsukami T, et al. Quantitative magnetic resonance imaging analysis of neovasculature volume in carotid atherosclerotic plaque. Circulation. 2003; 107(6):851–6. [PubMed: 12591755]
31. Kerwin WS, O'Brien KD, Ferguson MS, Polissar N, Hatsukami TS, Yuan C. Inflammation in carotid atherosclerotic plaque: a dynamic contrast-enhanced MR imaging study. Radiology. 2006; 241(2):459–68. [PubMed: 16966482]
32. Kerwin WS, Oikawa M, Yuan C, Jarvik GP, Hatsukami TS. MR imaging of adventitial vasa vasorum in carotid atherosclerosis. Magn Reson Med. 2008; 59(3):507–14. [PubMed: 18306402]
33. Dong L, Kerwin WS, Chen H, Chu B, Underhill HR, Neradilek MB, et al. Carotid artery atherosclerosis: effect of intensive lipid therapy on the vasa vasorum–evaluation by using dynamic contrast-enhanced MR imaging. Radiology. 2011; 260(1):224–31. [PubMed: 21493792]
34. Chen H, Ricks J, Rosenfeld M, Kerwin WS. Progression of experimental lesions of atherosclerosis: Assessment by kinetic modeling of black-blood dynamic contrast-enhanced MRI. Magn Reson Med. 2012
35. Calcagno C, Cornily JC, Hyafil F, Rudd JH, Briley-Saebo KC, Mani V, et al. Detection of neovessels in atherosclerotic plaques of rabbits using dynamic contrast enhanced MRI and 18F-FDG PET. Arterioscler Thromb Vasc Biol. 2008; 28(7):1311–7. [PubMed: 18467641]
36. Jesberger JA, Rafie N, Duerk JL, Sunshine JL, Mendez M, Remick SC, et al. Model-free parameters from dynamic contrast-enhanced-MRI: sensitivity to EES volume fraction and bolus timing. J Magn Reson Imaging. 2006; 24(3):586–94. [PubMed: 16892197]
37. Chaabane L, Pellet N, Bourdillon MC, Desbleds Mansard C, Sulaiman A, Hadour G, et al. Contrast enhancement in atherosclerosis development in a mouse model: in vivo results at 2 Tesla. MAGMA. 2004; 17(3–6):188–95. [PubMed: 15565504]
38. Alsaid H, De Souza G, Bourdillon MC, Chaubet F, Sulaiman A, Desbleds-Mansard C, et al. Biomimetic MRI contrast agent for imaging of inflammation in atherosclerotic plaque of ApoE(–/–)mice: a pilot study. Invest Radiol. 2009; 44(3):151–8. [PubMed: 19169144]
39. Calcagno C, Vucic E, Mani V, Goldschlager G, Fayad ZA. Reproducibility of black blood dynamic contrast-enhanced magnetic resonance imaging in aortic plaques of atherosclerotic rabbits. J Magn Reson Imaging. 32(1):191–198. [PubMed: 20578026]
40. Lobatto ME, Fayad ZA, Silvera S, Vucic E, Calcagno C, Mani V, et al. Multimodal clinical imaging to longitudinally assess a nanomedical anti-inflammatory treatment in experimental atherosclerosis. Mol Pharm. 2010; 7(6):2020–9. [PubMed: 21028895]

41. Lobatto ME, Calcagno C, Metselaar JM, Storm G, Stroes ES, Fayad ZA, et al. Imaging the efficacy of anti-inflammatory liposomes in a rabbit model of atherosclerosis by non-invasive imaging. Methods Enzymol. 2012; 508:211–28. [PubMed: 22449928]
42. Vucic E, Dickson SD, Calcagno C, Rudd JH, Moshier E, Hayashi K, et al. Pioglitazone modulates vascular inflammation in athero-sclerotic rabbits noninvasive assessment with FDG-PET-CT and dynamic contrast-enhanced MR imaging. JACC Cardiovasc Imaging. 2011; 4(10):1100–9. [PubMed: 21999870]
43. Vucic E, Calcagno C, Dickson SD, Rudd JH, Hayashi K, Bucerius J, et al. Regression of Inflammation in Atherosclerosis by the LXR Agonist R211945: A Noninvasive Assessment and Comparison With Atorvastatin. JACC Cardiovasc Imaging. 2012; 5(8):819–28. [PubMed: 22897996]
44. Fayad ZA, Mani V, Woodward M, Kallend D, Bansilal S, Pozza J, et al. Rationale and design of dal-PLAQUE: a study assessing efficacy and safety of dalcetrapib on progression or regression of atherosclerosis using magnetic resonance imaging and 18F-fluorodeoxyglucose positron emission tomography/computed tomography. Am Heart J. 2011; 162(2):214–221 e212. [PubMed: 21835280]
45. Fayad ZA, Mani V, Woodward M, Kallend D, Abt M, Burgess T, et al. Safety and efficacy of dalcetrapib on atherosclerotic disease using novel non-invasive multimodality imaging (dal-PLAQUE): a randomised clinical trial. Lancet. 2011; 378(9802):1547–59. [PubMed: 21908036]
46. Fang J, Nakamura H, Maeda H. The EPR effect: Unique features of tumor blood vessels for drug delivery, factors involved, and limitations and augmentation of the effect. Adv Drug Deliv Rev. 2011; 63(3):136–51. [PubMed: 20441782]
47. Lobbes MB, Miserus RJ, Heeneman S, Passos VL, Mutsaers PH, Debernardi N, et al. Atherosclerosis: contrast-enhanced MR imaging of vessel wall in rabbit model–comparison of gadofosveset and gadopentetate dimeglumine. Radiology. 2009; 250(3):682–91. [PubMed: 19244042]
48. Cornily JC, Hyafil F, Calcagno C, Briley-Saebo KC, Tunstead J, Aguinaldo JG, et al. Evaluation of neovessels in atherosclerotic plaques of rabbits using an albumin-binding intravascular contrast agent and MRI. J Magn Reson Imaging. 2008; 27(6):1406–11. [PubMed: 18504763]
49. Phinikaridou A, Andia ME, Protti A, Indermuehle A, Shah A, Smith A, et al. Noninvasive magnetic resonance imaging evaluation of endothelial permeability in murine atherosclerosis using an albumin-binding contrast agent. Circulation. 2012; 126(6):707–19. [PubMed: 22753191]
50. Lobbes MB, Heeneman S, Passos VL, Welten R, Kwee RM, van der Geest RJ, et al. Gadofosveset-enhanced magnetic resonance imaging of human carotid atherosclerotic plaques: a proof-of-concept study. Invest Radiol. 2010; 45(5):275–81. [PubMed: 20351652]
51. Sirol M, Moreno PR, Purushothaman KR, Vucic E, Amirbekian V, Weinmann HJ, et al. Increased neovascularization in advanced lipid-rich atherosclerotic lesions detected by gadofluorine-M-enhanced MRI: implications for plaque vulnerability. Circ Cardiovasc Imaging. 2009; 2(5):391–6. [PubMed: 19808627]
52. Barkhausen J, Ebert W, Heyer C, Debatin JF, Weinmann HJ. Detection of atherosclerotic plaque with Gadofluorine-enhanced magnetic resonance imaging. Circulation. 2003; 108(5):605–9. [PubMed: 12835227]
53. Ronald JA, Chen Y, Belisle AJ, Hamilton AM, Rogers KA, Hegele RA, et al. Comparison of gadofluorine-M and Gd-DTPA for noninvasive staging of atherosclerotic plaque stability using MRI. Circ Cardiovasc Imaging. 2009; 2(3):226–34. [PubMed: 19808597]
54. Zheng J, Ochoa E, Misselwitz B, Yang D, El Naqa I, Woodard PK, et al. Targeted contrast agent helps to monitor advanced plaque during progression: a magnetic resonance imaging study in rabbits. Invest Radiol. 2008; 43(1):49–55. [PubMed: 18097277]
55. Koktzoglou I, Harris KR, Tang R, Kane BJ, Misselwitz B, Weinmann HJ, et al. Gadofluorine-enhanced magnetic resonance imaging of carotid atherosclerosis in Yucatan miniswine. Invest Radiol. 2006; 41(3):299–304. [PubMed: 16481913]
56. Sirol M, Itskovich VV, Mani V, Aguinaldo JG, Fallon JT, Misselwitz B, et al. Lipid-rich atherosclerotic plaques detected by gadofluorine-enhanced in vivo magnetic resonance imaging. Circulation. 2004; 109(23):2890–6. [PubMed: 15184290]

57. Meding J, Urich M, Licha K, Reinhardt M, Misselwitz B, Fayad ZA, et al. Magnetic resonance imaging of atherosclerosis by targeting extracellular matrix deposition with Gadofluorine M. Contrast Media Mol Imaging. 2007; 2(3):120–9. [PubMed: 17557276]
58. Li D, Patel AR, Klibanov AL, Kramer CM, Ruiz M, Kang BY, et al. Molecular imaging of atherosclerotic plaques targeted to oxidized LDL receptor LOX-1 by SPECT/CT and magnetic resonance. Circ Cardiovasc Imaging. 2010; 3(4):464–72. [PubMed: 20442371]
59. Briley-Saebo KC, Shaw PX, Mulder WJ, Choi SH, Vucic E, Aguinaldo JG, et al. Targeted molecular probes for imaging atherosclerotic lesions with magnetic resonance using antibodies that recognize oxidation-specific epitopes. Circulation. 2008; 117(25):3206–15. [PubMed: 18541740]
60. Paulis LE, Jacobs I, van de Akker N, Geelen T, Molin D, Starmans LW, et al. Targeting of ICAM-1 on vascular endothelium under static and shear stress conditions using a liposomal Gd-based MRI contrast agent. J Nanobiotechnology. 2012; 10(1):25. [PubMed: 22716048]
61. Chaubet F, Bertholon I, Serfaty JM, Bazeli R, Alsaid H, Jandrot-Perrus M, et al. A new macromolecular paramagnetic MR contrast agent binds to activated human platelets. Contrast Media Mol Imaging. 2007; 2(4):178–88. [PubMed: 17828728]
62. Winter PM, Neubauer AM, Caruthers SD, Harris TD, Robertson JD, Williams TA, et al. Endothelial alpha(v)beta3 integrin-targeted fumagillin nanoparticles inhibit angiogenesis in atherosclerosis. Arterioscler Thromb Vasc Biol. 2006; 26(9):2103–9. [PubMed: 16825592]
63. Winter PM, Morawski AM, Caruthers SD, Fuhrhop RW, Zhang H, Williams TA, et al. Molecular imaging of angiogenesis in early-stage atherosclerosis with alpha(v)beta3-integrin-targeted nanoparticles. Circulation. 2003; 108(18):2270–4. [PubMed: 14557370]
64. Winter PM, Caruthers SD, Zhang H, Williams TA, Wickline SA, Lanza GM. Antiangiogenic synergism of integrin-targeted fumagillin nanoparticles and atorvastatin in atherosclerosis. JACC Cardiovasc Imaging. 2008; 1(5):624–34. [PubMed: 19356492]
65. Winter PM, Caruthers SD, Allen JS, Cai K, Williams TA, Lanza GM, et al. Molecular imaging of angiogenic therapy in peripheral vascular disease with alphanubeta3-integrin-targeted nanoparticles. Magn Reson Med. 2010; 64(2):369–76. [PubMed: 20665780]
66. Burtea C, Laurent S, Murariu O, Rattat D, Toubeau G, Verbruggen A, et al. Molecular imaging of alpha v beta3 integrin expression in atherosclerotic plaques with a mimetic of RGD peptide grafted to Gd-DTPA. Cardiovasc Res. 2008; 78(1):148–57. [PubMed: 18174291]
67. Mulder WJ, Strijkers GJ, Briley-Saboe KC, Frias JC, Aguinaldo JG, Vucic E, et al. Molecular imaging of macrophages in atherosclerotic plaques using bimodal PEG-micelles. Magn Reson Med. 2007; 58(6):1164–70. [PubMed: 18046703]
68. Amirbekian V, Lipinski MJ, Briley-Saebo KC, Amirbekian S, Aguinaldo JG, Weinreb DB, et al. Detecting and assessing macrophages in vivo to evaluate atherosclerosis noninvasively using molecular MRI. Proc Natl Acad Sci U S A. 2007; 104(3):961–6. [PubMed: 17215360]
69. Lipinski MJ, Frias JC, Amirbekian V, Briley-Saebo KC, Mani V, Samber D, et al. Macrophage-specific lipid-based nanoparticles improve cardiac magnetic resonance detection and characterization of human atherosclerosis. JACC Cardiovasc Imaging. 2009; 2(5):637–47. [PubMed: 19442953]
70. Maiseyeu A, Mihai G, Roy S, Kherada N, Simonetti OP, Sen CK, et al. Detection of macrophages via paramagnetic vesicles incorporating oxidatively tailored cholesterol ester: an approach for atherosclerosis imaging. Nanomedicine (Lond). 2010; 5(9):1341–56. [PubMed: 21128718]
71. Maiseyeu A, Mihai G, Kampfrath T, Simonetti OP, Sen CK, Roy S, et al. Gadolinium-containing phosphatidylserine liposomes for molecular imaging of atherosclerosis. J Lipid Res. 2009; 50(11): 2157–63. [PubMed: 19017616]
72. Yamakoshi Y, Qiao H, Lowell AN, Woods M, Paulose B, Nakao Y, et al. LDL-based nanoparticles for contrast enhanced MRI of atheroplaques in mouse models. Chem Commun (Camb). 2011; 47(31):8835–7. [PubMed: 21743892]
73. Frias JC, Williams KJ, Fisher EA, Fayad ZA. Recombinant HDL-like nanoparticles: a specific contrast agent for MRI of atherosclerotic plaques. J Am Chem Soc. 2004; 126(50):16316–7. [PubMed: 15600321]

74. Frias JC, Ma Y, Williams KJ, Fayad ZA, Fisher EA. Properties of a versatile nanoparticle platform contrast agent to image and characterize atherosclerotic plaques by magnetic resonance imaging. Nano Lett. 2006; 6(10):2220–4. [PubMed: 17034087]
75. Cormode DP, Chandrasekar R, Delshad A, Briley-Saebo KC, Calcagno C, Barazza A, et al. Comparison of synthetic high density lipoprotein (HDL) contrast agents for MR imaging of atherosclerosis. Bioconjug Chem. 2009; 20(5):937–43. [PubMed: 19378935]
76. Schmitz SA, Taupitz M, Wagner S, Wolf KJ, Beyersdorff D, Hamm B. Magnetic resonance imaging of atherosclerotic plaques using superparamagnetic iron oxide particles. J Magn Reson Imaging. 2001; 14(4):355–61. [PubMed: 11599058]
77. Schmitz SA, Coupland SE, Gust R, Winterhalter S, Wagner S, Kresse M, et al. Superparamagnetic iron oxide-enhanced MRI of atherosclerotic plaques in Watanabe hereditable hyperlipidemic rabbits. Invest Radiol. 2000; 35(8):460–71. [PubMed: 10946973]
78. Kooi ME, Cappendijk VC, Cleutjens KB, Kessels AG, Kitslaar PJ, Borgers M, et al. Accumulation of ultrasmall superparamagnetic particles of iron oxide in human atherosclerotic plaques can be detected by in vivo magnetic resonance imaging. Circulation. 2003; 107(19):2453–8. [PubMed: 12719280]
79. Tang TY, Howarth SP, Miller SR, Graves MJ, Patterson AJ, JMUK I, Li ZY, et al. The ATHEROMA (Atorvastatin Therapy: Effects on Reduction of Macrophage Activity) Study. Evaluation using ultrasmall superparamagnetic iron oxide-enhanced magnetic resonance imaging in carotid disease. J Am Coll Cardiol. 2009; 53(22):2039–50. [PubMed: 19477353]
80. van Tilborg GA, Vucic E, Strijkers GJ, Cormode DP, Mani V, Skajaa T, et al. Annexin A5-functionalized bimodal nanoparticles for MRI and fluorescence imaging of atherosclerotic plaques. Bioconjug Chem. 2010; 21(10):1794–803. [PubMed: 20804153]
81. Burtea C, Laurent S, Lancelot E, Ballet S, Murariu O, Rousseaux O, et al. Peptidic targeting of phosphatidylserine for the MRI detection of apoptosis in atherosclerotic plaques. Mol Pharm. 2009; 6(6):1903–19. [PubMed: 19743879]
82. Chen JW, Pham W, Weissleder R, Bogdanov A Jr. Human myeloperoxidase: a potential target for molecular MR imaging in atherosclerosis. Magn Reson Med. 2004; 52(5):1021–8. [PubMed: 15508166]
83. Querol M, Chen JW, Bogdanov AA Jr. A paramagnetic contrast agent with myeloperoxidase-sensing properties. Org Biomol Chem. 2006; 4(10):1887–95. [PubMed: 16688334]
84. Ronald JA, Chen JW, Chen Y, Hamilton AM, Rodriguez E, Reynolds F, et al. Enzyme-sensitive magnetic resonance imaging targeting myeloperoxidase identifies active inflammation in experimental rabbit atherosclerotic plaques. Circulation. 2009; 120(7):592–9. [PubMed: 19652086]
85. von Bary C, Makowski M, Preissel A, Keithahn A, Warley A, Spuentrup E, et al. MRI of coronary wall remodeling in a swine model of coronary injury using an elastin-binding contrast agent. Circ Cardiovasc Imaging. 2011; 4(2):147–55. [PubMed: 21378029]
86. Makowski MR, Preissel A, von Bary C, Warley A, Schachoff S, Keithan A, et al. Three-dimensional imaging of the aortic vessel wall using an elastin-specific magnetic resonance contrast agent. Invest Radiol. 2012; 47(7):438–44. [PubMed: 22627945]
87. Beilvert A, Vassy R, Canet-Soulas E, Rousseaux O, Picton L, Letourneur D, et al. Synthesis and evaluation of a trityrosine decorated dextran MR contrast agent for vulnerable plaque detection. Chem Commun (Camb). 2011; 47(19):5506–8. [PubMed: 21455511]
88. Beilvert A, Cormode DP, Chaubet F, Briley-Saebo KC, Mani V, Mulder WJ, et al. Tyrosine polyethylene glycol (PEG)-micelle magnetic resonance contrast agent for the detection of lipid rich areas in atherosclerotic plaque. Magn Reson Med. 2009; 62(5):1195–201. [PubMed: 19780153]
89. Lancelot E, Amirbekian V, Brigger I, Raynaud JS, Ballet S, David C, et al. Evaluation of matrix metalloproteinases in atherosclerosis using a novel noninvasive imaging approach. Arterioscler Thromb Vasc Biol. 2008; 28(3):425–32. [PubMed: 18258820]
90. Hyafil F, Vucic E, Cornily JC, Sharma R, Amirbekian V, Blackwell F, et al. Monitoring of arterial wall remodelling in atherosclerotic rabbits with a magnetic resonance imaging contrast agent binding to matrix metalloproteinases. Eur Heart J. 2011; 32(12):1561–71. [PubMed: 21118852]

91. Ouimet T, Lancelot E, Hyafil F, Rienzo M, Deux F, Lemaitre M, et al. Molecular and cellular targets of the MRI contrast agent P947 for atherosclerosis imaging. Mol Pharm. 2012; 9(4):850–61. [PubMed: 22352457]
92. Flacke S, Fischer S, Scott MJ, Fuhrhop RJ, Allen JS, McLean M, et al. Novel MRI contrast agent for molecular imaging of fibrin: implications for detecting vulnerable plaques. Circulation. 2001; 104(11):1280–5. [PubMed: 11551880]
93. Winter PM, Caruthers SD, Yu X, Song SK, Chen J, Miller B, et al. Improved molecular imaging contrast agent for detection of human thrombus. Magn Reson Med. 2003; 50(2):411–6. [PubMed: 12876719]
94. Botnar RM, Buecker A, Wiethoff AJ, Parsons EC Jr, Katoh M, Katsimaglis G, et al. In vivo magnetic resonance imaging of coronary thrombosis using a fibrin-binding molecular magnetic resonance contrast agent. Circulation. 2004; 110(11):1463–6. [PubMed: 15238457]
95. Sirol M, Aguinaldo JG, Graham PB, Weisskoff R, Lauffer R, Mizsei G, et al. Fibrin-targeted contrast agent for improvement of in vivo acute thrombus detection with magnetic resonance imaging. Atherosclerosis. 2005; 182(1):79–85. [PubMed: 16115477]
96. Sirol M, Fuster V, Badimon JJ, Fallon JT, Moreno PR, Toussaint JF, et al. Chronic thrombus detection with in vivo magnetic resonance imaging and a fibrin-targeted contrast agent. Circulation. 2005; 112(11):1594–600. [PubMed: 16145001]
97. Makowski MR, Forbes SC, Blume U, Warley A, Jansen CH, Schuster A, et al. In vivo assessment of intraplaque and endothelial fibrin in ApoE(−/−) mice by molecular MRI. Atherosclerosis. 2012; 222(1):43–9. [PubMed: 22284956]
98. Cormode DP, Jarzyna PA, Mulder WJ, Fayad ZA. Modified natural nanoparticles as contrast agents for medical imaging. Adv Drug Deliv Rev. 62(3):329–338. [PubMed: 19900496]
99. Tang, J.; R, D.; Izquierdo-Garcia, D.; Cormode, DP.; Stroes, ES.; Lobatto, ME.; Kuan, EL.; Randolph, GL.; Fuster, V.; Fisher, EA.; Mulder, WJ.; Fayad, ZA. Abstract 9601: A Statin-Loaded Nanotherapy Increases Anti-Inflammatory Effects of Statin on Atherosclerosis. Orlando, Florida, USA: 2011.
100. Rudd JH, Myers KS, Bansilal S, Machac J, Pinto CA, Tong C, et al. Atherosclerosis inflammation imaging with 18F-FDG PET: carotid, iliac, and femoral uptake reproducibility, quantification methods, and recommendations. J Nucl Med. 2008; 49(6):871–8. [PubMed: 18483100]
101. Rudd JH, Elkhawad M, Fayad ZA. Vascular imaging with 18F-FDG PET/CT: optimal 18F-FDG circulation time? J Nucl Med. 2009; 50(9):1560. [PubMed: 19690022]
102. Tawakol A, Migrino RQ, Bashian GG, Bedri S, Vermylen D, Cury RC, et al. In vivo 18F-fluorodeoxyglucose positron emission tomography imaging provides a noninvasive measure of carotid plaque inflammation in patients. J Am Coll Cardiol. 2006; 48(9):1818–24. [PubMed: 17084256]
103. Tahara N, Kai H, Yamagishi S, Mizoguchi M, Nakaura H, Ishibashi M, et al. Vascular inflammation evaluated by [18F]-fluorodeoxyglucose positron emission tomography is associated with the metabolic syndrome. J Am Coll Cardiol. 2007; 49(14):1533–9. [PubMed: 17418291]
104. Tahara N, Kai H, Nakaura H, Mizoguchi M, Ishibashi M, Kaida H, et al. The prevalence of inflammation in carotid atherosclerosis: analysis with fluorodeoxyglucose-positron emission tomography. Eur Heart J. 2007; 28(18):2243–8. [PubMed: 17681956]
105. Tahara N, Kai H, Ishibashi M, Nakaura H, Kaida H, Baba K, et al. Simvastatin attenuates plaque inflammation: evaluation by fluorodeoxyglucose positron emission tomography. J Am Coll Cardiol. 2006; 48(9):1825–31. [PubMed: 17084257]
106. Cyran CC, Sourbron S, Bochmann K, Habs M, Pfefferkorn T, Rominger A, et al. Quantification of supra-aortic arterial wall inflammation in patients with arteritis using high resolution dynamic contrast-enhanced magnetic resonance imaging: initial results in correlation to [18F]-FDG PET/CT. Invest Radiol. 2011; 46(9):594–9. [PubMed: 21577125]
107. Lipinski MJ, Amirbekian V, Frias JC, Aguinaldo JG, Mani V, Briley-Saebo KC, et al. MRI to detect atherosclerosis with gadolinium-containing immunomicelles targeting the macrophage scavenger receptor. Magn Reson Med. 2006; 56(3):601–10. [PubMed: 16902977]

108. Amirbekian V, Aguinaldo JG, Amirbekian S, Hyafil F, Vucic E, Sirol M, et al. Atherosclerosis and matrix metalloproteinases: experimental molecular MR imaging in vivo. Radiology. 2009; 251(2):429–38. [PubMed: 19224894]

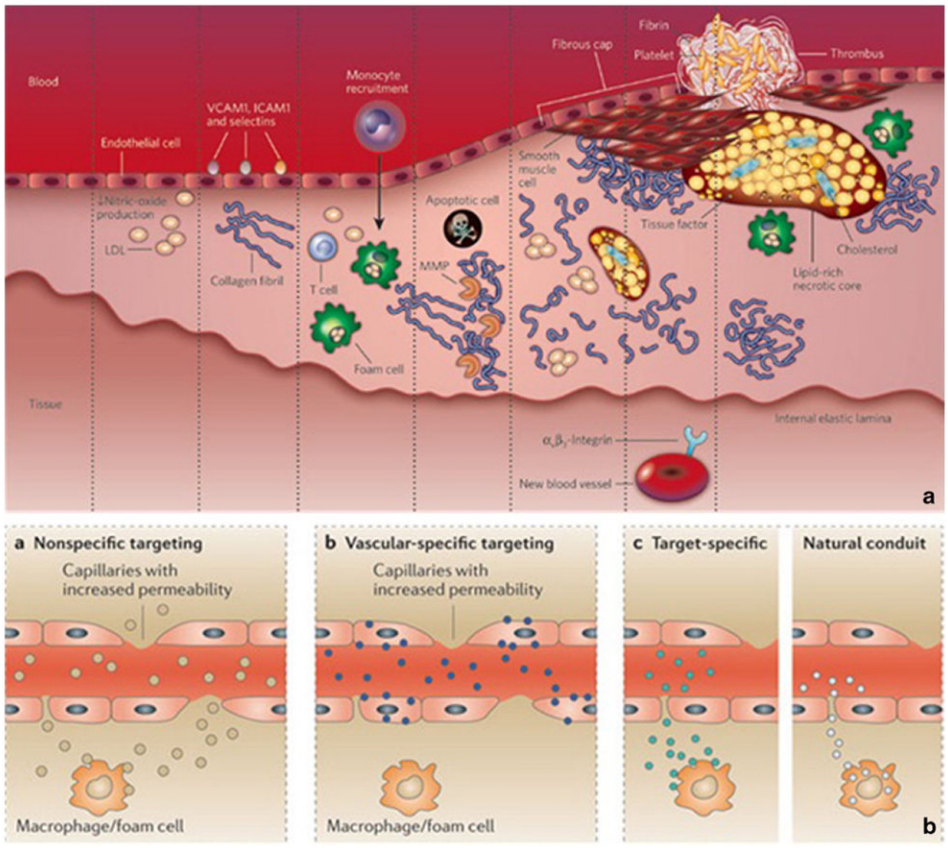

Fig. 1.

Atherosclerosis cascade and targeting mechanisms for contrast agents. **a**, atherosclerosis cascade. **b**, mechanisms of delivery of targeted and non-targeted agents for atherosclerosis. Panel **a** was reprinted with permission from Nature. 2008 Feb 21;451(7181):953–7. Panel **b** was reprinted with permission from Nat Rev Drug Discov. 2011 Oct 21;10(11):835–52

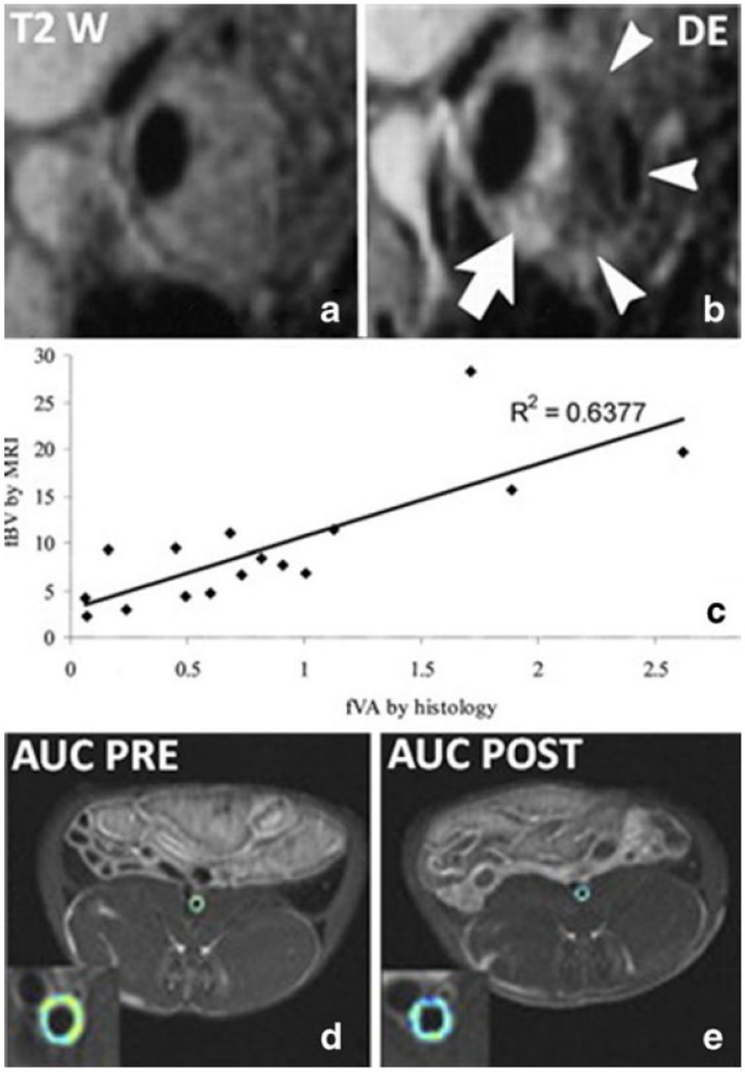

Fig. 2.

Example of application of non-targeted gadolinium based contrast agents. **a**, T2 weighted image of stenotic human carotid plaque. **b**, T1 weighted post-contrast image of the same plaque shown in **a**. The white arrows indicate highly enhancing regions in adventitia and fibrous cap. The dark non-enhancing region is a lipid core, which is not visible without contrast in the T2 weighted image in **a. c**, correlation between plaque neovascularization by histology and fractional plasma volume calculated by DCE-MRI of carotid atherosclerosis. **d** and **e**, area under the curve (AUC) calculated by DCE-MRI in the aorta of a representative atherosclerotic rabbit before (**d**) and after (**e**) treatment with pioglitazone. The colder colors of the AUC map in panel **e** indicate a reduction of neovessels/permeability after treatment. Panel **a** and **b** were reprinted with permission from Radiology. 2002 May;223 (2):566-73. Panel **c** was reprinted with permission from Circulation. 2003 Feb 18;107(6):851–6. Panels **d** and **e** were reprinted with permission from JACC Cardiovasc Imaging. 2011 Oct;4(10): 1100–9

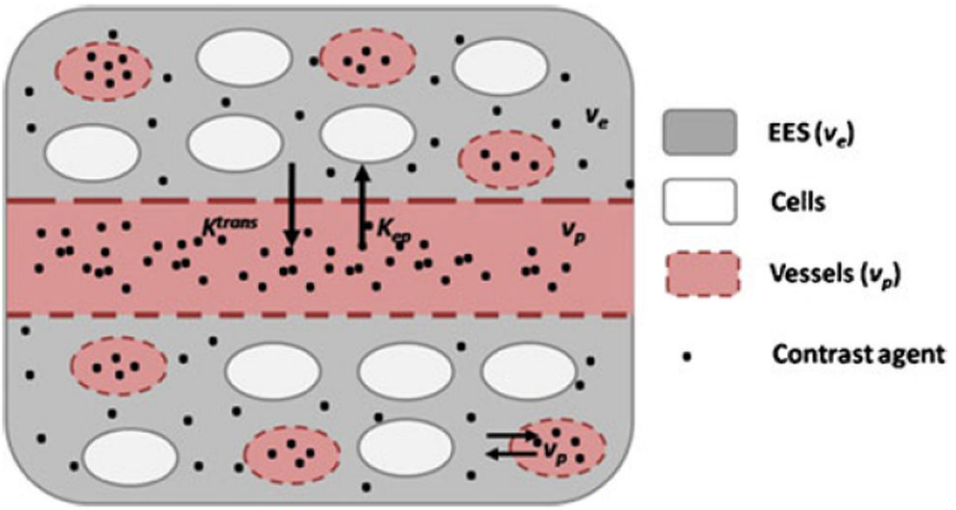

Fig. 3.

Schematics of the extravasation of non-specific non-targeted contrast agents into the atherosclerotic vessel wall. The contrast agent (black dots) is in the vasculature (red, v_p) and leaks into the extra-vascular extra-cellular space (EES, v_e in gray) through the permeable endothelium, but does not enter cells (white). The contrast agent enters with kinetic constant K^{trans} and flows back into the vessels with constant K_{ep}

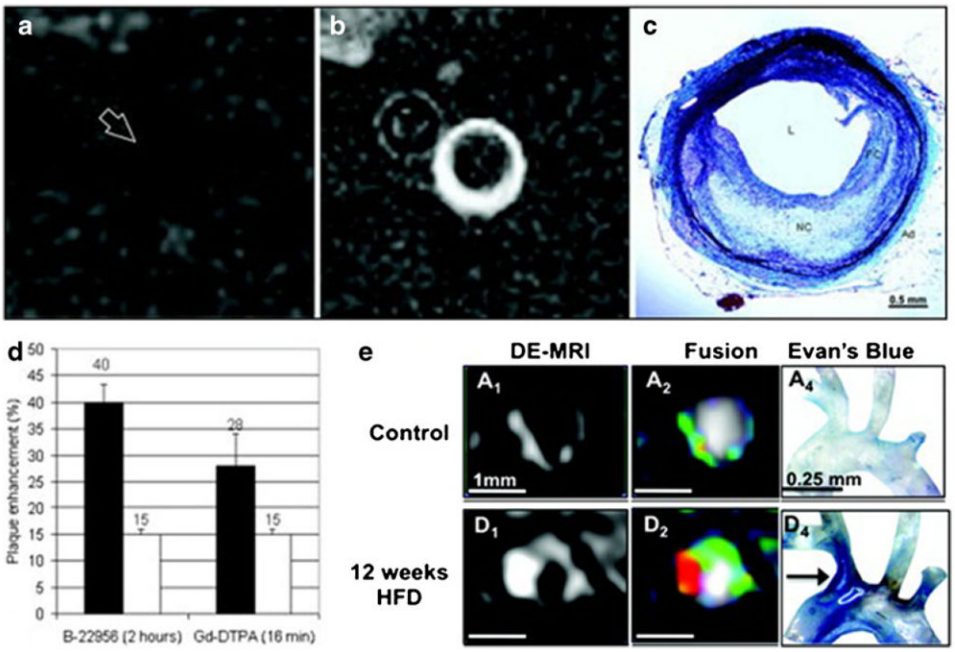

Fig. 4.

Examples of non-specific targeted gadolinium based contrast agents. a and b, MR imaging before (**a**) and after (**b**) injection of gadofluorine M in the abdominal aorta of atherosclerotic rabbits. **c**, corresponding histological section stained with combined Masson elastin trichrome. The atherosclerotic plaque is rich in lipids, matching the enhancement seen with gadofluorine M. **d**, signal enhancement after the injection of an intravascular albumin binding contrastagent (B-22956) and Gd-DTPA. Black bars, atherosclerotic rabbits. White bars, control rabbits. The intravascular agent shows more pronounced enhancement with respect to Gd-DTPA. **e**, MRI showing uptake of gadofosveset in the brachiocephalic artery of control (upper row) and ApoE –/– mice(lower row). Higher uptake is seen in ApoE –/– mice, as it is demonstrated by the Evan's blue staining (third column). Panels **a, b** and **c** were reprinted with permission from Circ Cardiovasc Imaging. 2009 Sep;2(5):391–6. Panel **d** was reprinted with permission from Arterioscler Thromb Vasc Biol. 2008 Jul;28(7):1311–7. Panel **e** was reprinted with permission from Circulation. 2012 Aug 7;126(6):707–19

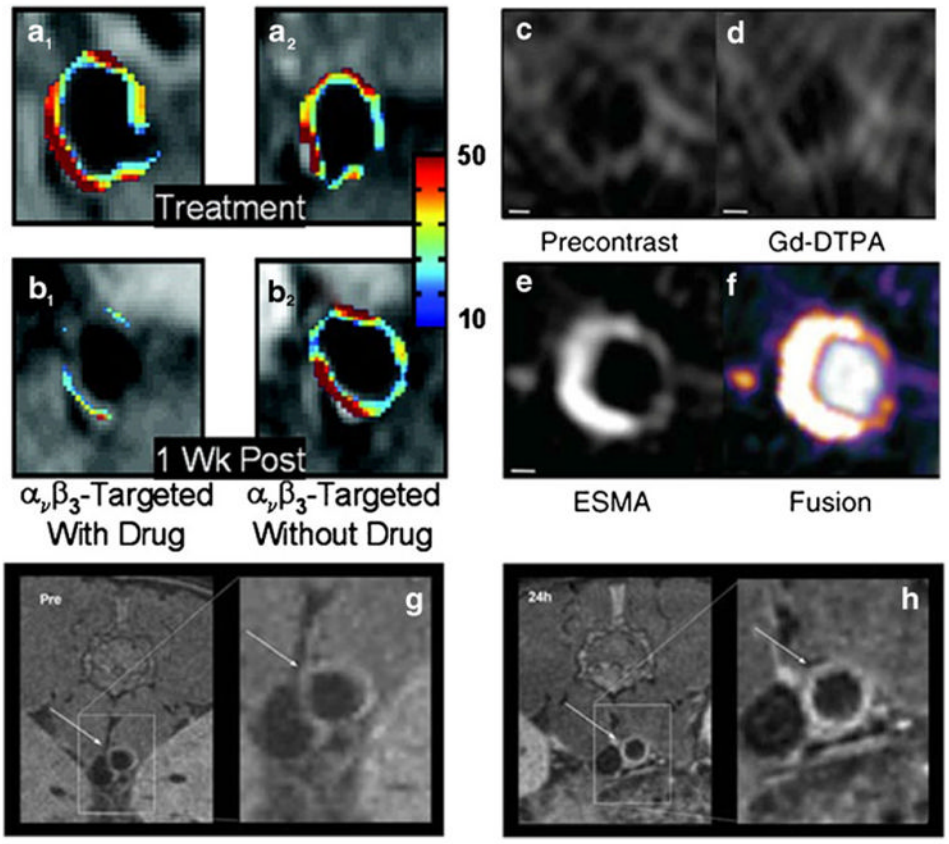

Fig. 5.

Examples of imaging with specific targeted gadolinium based contrast agents. **a** and **b**, imaging with Gd based αvβ3 targeted agent before (**a**) and after (**b**) injection of particles with (column 1) or without (column 2) fumagallin, and anti-angiogenic agent. After injection of αvβ3 with fumagallin significantly less enhancement can be seen in the aorta of cholesterol fed rabbits. **c-f**, targeting of elastin in the vessel wall of the brachiocephalic artery of *ApoE*$^{-/-}$ mice. The elastin binding contrast agent (ESMA) shows higher enhancement than Gd-DTPA. **g** and **h**, MRI images of the abdominal aorta of ApoE –/– mice, indicated by arrows, before (**g**) and after (**h**) injection with reconstituted Gd labeled HDL nanoparticles for targeting of macrophages in the abdominal aorta of atherosclerotic rabbits. Panels **a** and **b** were reprinted with permission from Arterioscler Thromb Vasc Biol. 2006 Sep;26 (9):2103–9. Panel **c-f** were reprinted with permission from Nat Med. 2011 Mar; 17(3):383–8. Panels **g** and **h** were reprinted with permission from Small. 2008 Sep;4(9): 1437–44

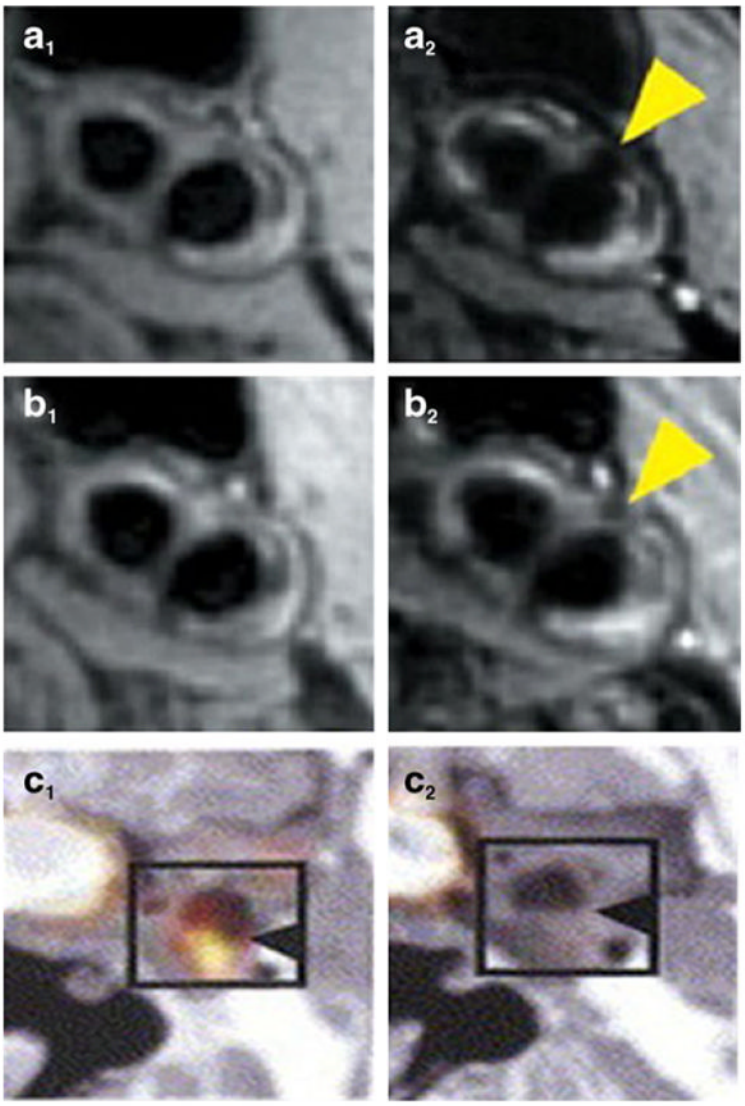

Fig. 6.

Examples of other imaging modalities that target specific processes in the atherosclerotic cascade. **a** and **b**, usage of ultra-small iron oxide particles (USPIO) to target plaque inflammation before (column 1) and after (column 2) low dose statin treatment as part of the ATHEROMA study. **c**, decrease in FDG signal before and after statin treatment in human subject with carotid atherosclerosis. Panels **a** and **b** were reprinted with permission from J Am Coll Cardiol. 2009 Jun 2;53(22):2039–50. Panel **c** was reprinted with permission from J Am Coll Cardiol. 2006 Nov 7;48(9):1825–31

Table 1

Summary of most important molecular targets of gadolinium based specific targeted contrast agents

	Medium	Author	Species	Areas of accumulation
Oxidized lipoproteins	Molecular probe targeted at oxidized LDL receptor LOX-1	Li et al. [58]	LDLR(−/−) mice	Plaque shoulder
	Micelles with antibodies against oxidation-specific epitopes	Saebo et al. [59]	ApoE(−/−) mice	Macrophages rich areas
Adhesion molecules	Liposomes with anti ICAM-1 antibodies	Paulis et al. [60]	In vitro	Cells activated by TNF-alfa
	Gd-DOTA with chemical groups interacting with P-selectin	Alsaid et al. [38]	ApoE(−/−) mice	Abdominal aortic wall
	Agent targeted to the integrin αvβ3	Winter et al. [62-65]	Rabbits	Plaque neovascularization
		Burtea et al. [66]	ApoE(−/−) mice	
Macrophages	Immunomicelles and nanoparticles targeted against the macrophage scavenger receptor	Amirbekian et al. [68]	ApoE(−/−) mice	Macrophages rich area
		Mulder et al. [67]		
		Lipsinki et al. [107]		
	Phosphatidylserine vesicles	Maiseyeu et al. [70, 71]	Rabbits	Colocalization with macrophages
	Lipoprotein based particles (LDL, HDL)	Yamakoshi et al. [72]	ApoE(−/−) mice	Macrophages
		Frias et al. [73, 74]		
		Cormode et al. [75]		
Apopoptic cells	Annexin 5 targeted nanoparticle	van Tilborg et al. [80]	ApoE(−/−) mice	Abdominal aortic wall
	Liposomes enriched with phosphatidylserine	Malaseyeu et al. [71]	In vitro	Macrophages
	Phosphatidylserine-specific peptide	Burtea et al. [81]	ApoE(−/−) mice	Abdominal aortic wall
Myeloperoxydase	Paramagnetic electron donor compound conjugated to Gd-DOTA	Chen et al. [82]	In vitro	Colocalizes with myelopreoxydase activity in enzyme solutions and in a model tissue-like system
	Modified Gd based agent as a paramagnetic sensor of MPO enzymatic activity	Querol et al. [83]	Mice	Signal enhancement in implants containing human MPO
	Myeloperoxidase sensor bis-5HT-DTPA(Gd) [MPO(Gd)]	Ronald et al. [84]	NZW Rabbits	Colocalizes with myeloperoxidase-rich areas infiltrated by macrophages
Extra-cellular matrix	Elastin-binding contrast agent (BMS-753951)	Von Bary et al. [85]	Pigs (coronary arteries)	Coronary, aorta and pulmonary arteries vessel wall
	Elastin-specific magnetic resonance contrast agent (ESMA)	Makovski et al. [86]	Pigs (throracic aortas)	Colocalizes with elastic fibers confirmed by electron microscopy
	Gd polyethylene glycol (PEG)-micelles functionalized with tyrosine residues	Beilvert et al. [87, 88]	ApoE(−/−) mice	Colocalizes with lipid-rich areas
Matrix metalloproteinases	P947	Lancelot et al. [89]	In vitro and ApoE(−/−) mice	Preferential uptake in MMP-rich with respect to MMP-poor plaques

	Medium	Author	Species	Areas of accumulation
		Amirbekian et al. [108]		
		Hyafil et al. [90]	Rabbits	Colocalized with MMP-2 activity
		Ouimet et al. [91]	Ex vivo	Colocalizes with areas rich in MMPs, angiotensin converting enzyme (ACE) and aminopeptidases N (APN)
Fibrin	Gd based agent (Gd-DTPA-BOA)	Flacke et al. [92]	In vitro	Colocalizes with fibrin rich areas
	Gd-DTPA-phosphatidylethanolamine (PE) with anti-fibrin antibodies	Winter et al. [93]	In vitro	
	EP-2104R	Botnar et al. [94]	Swines	Injured carotid arteries regardless of their size, location, and age
	EP-1242	Sirol et al. [95, 96]	Guinea pigs	
	EP-1240		Rabbits	
	FTCA	Makowski et al. [97]	ApoE(−/−) mice	Brachiocephalic arteries